

Plasmon Generation by Excitons in Carbon Nanotubes

I.V. Bondarev and T. Antonijevich

Physics Department, North Carolina Central University
1801 Fayetteville Str, Durham, NC 27707, USA, ibondarev@ncsu.edu

ABSTRACT

We theoretically demonstrate the possibility of low-energy localized surface plasmon generation by optically excited excitons in small-diameter (~ 1 nm) single wall carbon nanotubes. The stimulated character of such a non-radiative energy transfer causes the buildup of the macroscopic population numbers of plasmons associated with high-intensity coherent optical-frequency fields localized at nanoscale throughout the nanotube surface. The effect can be used for various applications, such as near-field nonlinear-optical probing, switching, or materials nanoscale modification.

Keywords: single wall carbon nanotubes, excitons, plasmons, coherent optical effects

1 INTRODUCTION

The true potential of carbon nanotube (CN) based optoelectronic device applications lies in the ability to tune their properties in a precisely controllable way. In particular, optical properties of semiconducting CNs originate from excitons [1], [2], and may be tuned by either electrostatic doping [3], [4], or by means of the quantum confined Stark effect (QCSE) with an electrostatic field applied perpendicular to the CN axis [5], [6]. In both cases the exciton properties are mediated by collective plasmon excitations in CNs [7]. In the case of the perpendicular electrostatic field applied, we have shown recently that the QCSE allows one to control exciton-interband-plasmon coupling in individual undoped CNs and their optical absorption properties, both linear [5], [6] and non-linear [8], accordingly.

Here, we extend our studies to demonstrate the possibility of low-energy localized surface plasmon generation by optically excited excitons in individual small-diameter (~ 1 nm) carbon nanotubes [9]. The phenomenon is pretty much similar to the SPACER effect (Surface Plasmon Amplification by Stimulated Emission of Radiation) reported earlier for a number of hybrid metal-semiconductor-dielectric nanosystems [10].

Plasmons are coherent charge density waves due to the periodic opposite phase displacements of the electron shells with respect to the ion cores. In general, plasmons cannot be excited by light in optical absorption

since they are longitudinal excitations while photons are transverse. In small-diameter semiconducting CNs, light polarized along the nanotube axis excites excitons which, in turn, can couple to the nearest (same-band) interband plasmons [6]. Both of these collective excitations originate from the same electronic transitions and, therefore, occur at the same (relatively low) energies ~ 1 eV, as opposed to bulk semiconductors where they are separated in energy by tens of eVs. Their coexistence in the same energy range in carbon nanotubes is a unique feature of the confined quasi-1D geometry where the transverse electronic motion is quantized to form 1D bands and the longitudinal motion is continuous.

The stimulated character of the non-radiative energy transfer, whereby the external electromagnetic (EM) radiation absorbed to excite excitons transfers into the energy of surface plasmons, can efficiently mediate and greatly enhance the electromagnetic absorption by pristine semiconducting nanotubes, to result in the buildup of the macroscopic population numbers of coherent surface plasmons associated with high-intensity coherent oscillating electric fields concentrated locally throughout the nanotube length. The effect can manifest itself both in individual CNs and in densely packed aligned nanotube films. The strong local coherent fields produced in this way can be used in a variety of new tunable optoelectronic applications of carbon nanotubes, such as near-field non-linear optical probing and sensing, optical switching, enhanced electromagnetic absorption, and materials nanoscale modification. The process can be controlled via the QCSE, by means of an electrostatic field applied perpendicular to the nanotube axis.

2 BRIEF SKETCH OF THE MODEL

In small-diameter semiconducting CNs, because of their quasi-one-dimensionality, excitons are excited by the external EM radiation polarized along the CN axis [6]. As a consequence, they have their transition dipole moment and translational quasi-momentum both directed along the nanotube axis (longitudinal excitons). That is why they are able to couple to their neighboring (low-energy, interband) longitudinal plasmon modes (Fig. 1, top panel). When the exciton is excited and the nanotube's surface EM field subsystem is in the vacuum

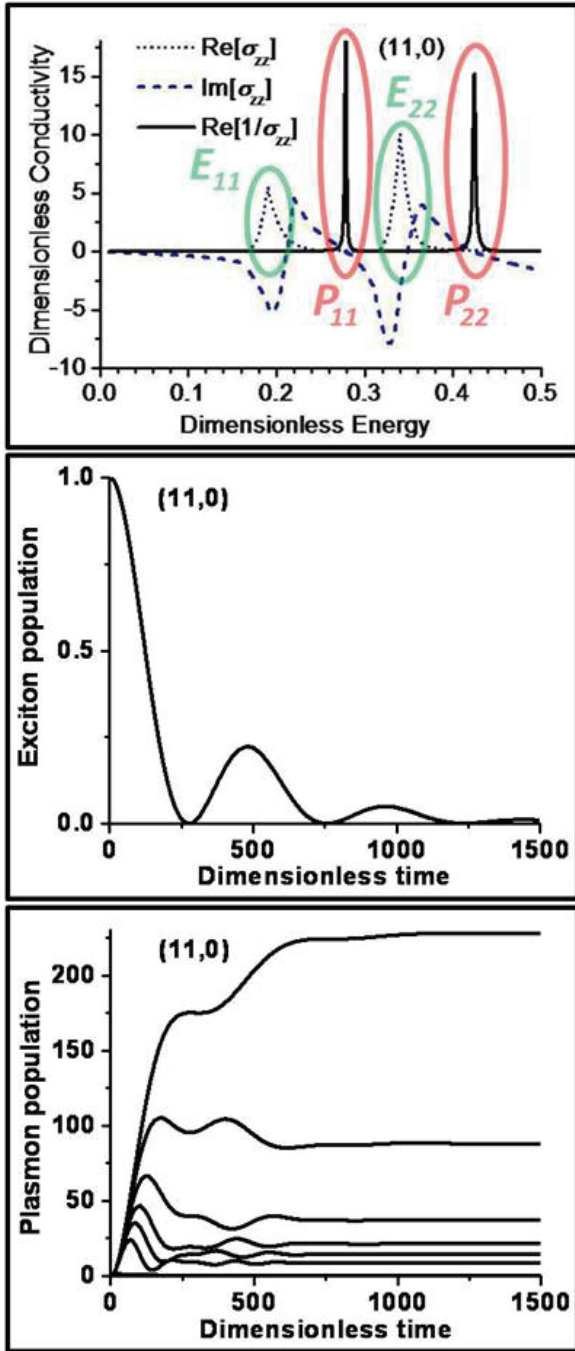


Figure 1: Calculations for the (11,0) CN. *Top*: Energy dependence of the dimensionless (normalized by $e^2/2\pi\hbar$) axial surface conductivity of the nanotube. Ovals indicate the lowest-energy exciton (E_{ii}) and plasmon (P_{ii}) excitations (given by the peaks of $\text{Re}[\sigma_{zz}]$ and $\text{Re}[1/\sigma_{zz}]$, respectively). *Middle*: Calculated time dependence of the first bright exciton (E_{11}) population probability, when the exciton energy is close to the nearest plasmon resonance (P_{11}). *Bottom*: Same for the plasmon P_{11} as the first bright exciton energy is tuned close to it (higher lines correspond to smaller de-tunings with E_{11} always being less than P_{11}). Dimensionless time and energy are defined as $[Time]2\gamma_0/\hbar$ and $[Energy]/2\gamma_0$, respectively, where $\gamma_0 = 2.7$ eV is the C-C overlap integral.

state, the time-dependent wave function of the whole system "exciton + surface EM field" is of the form (only the first bright exciton is considered here for simplicity, corresponding to the E_{11} peak of $\text{Re}[\sigma_{zz}]$ in the top panel of Fig. 1; see Ref. [6] for more details)

$$|\psi(t)\rangle = \sum_{\mathbf{k}} C_{ex}(\mathbf{k}, t) e^{-i(E(\mathbf{k})-i\Delta E)t/\hbar} |1(\mathbf{k})\rangle_{ex} |0\rangle_p + \sum_{\mathbf{k}} \int_0^\infty d\omega C_p(\mathbf{k}, \omega, t) e^{-i\omega t} |0\rangle_{ex} |1(\mathbf{k}, \omega)\rangle_p$$

Here, $|1(\mathbf{k})\rangle_{ex}$ is the excited single-quantum Fock state with one exciton and $|1(\mathbf{k}, \omega)\rangle$ is that with one surface EM mode excited (plasmon) of frequency ω . The exciton relaxation constant ΔE is normally attributed to the exciton-phonon scattering [11]. The vacuum states are $|0\rangle_{ex}$ and $|0\rangle_p$ for the exciton subsystem and field subsystem, respectively. The coefficients $C_{ex}(\mathbf{k}, t)$ and $C_p(\mathbf{k}, \omega, t)$ stand for the population probability amplitudes of the respective states of the whole system. They are found from the set of the two coupled simultaneous differential equations, which under resonance conditions (exciton energy is close to the plasmon resonance energy) results in

$$|C_p(\beta)|^2 \approx \frac{1}{2\pi} \bar{\Gamma}_0(x_p) \rho(x_p) \left| \int_0^\beta d\beta' C_{ex}(\beta') e^{i(x_p - \varepsilon + i\Delta\varepsilon)\beta'} \right|^2$$

Here, all quantities are dimensionless, normalized to $2\gamma_0$, with $\gamma_0 = 2.7$ eV being the C-C overlap integral. The coefficient on front of the integral is the exciton spontaneous decay rate into plasmons taken at the plasmon resonance energy x_p , with $\rho(x)$ representing the (sharply peaked) plasmon density of states (DOS – see Fig. 1, top panel). The condition $\varepsilon \approx x_p$ is assumed to hold, whereby the exciton population probability amplitude can be approximated as

$$C_{ex}(\beta) \approx \frac{1}{2} \left(1 + \frac{\delta x}{\sqrt{\delta x^2 - X^2}} \right) e^{-(\delta x - \sqrt{\delta x^2 - X^2})\beta/2} + \frac{1}{2} \left(1 - \frac{\delta x}{\sqrt{\delta x^2 - X^2}} \right) e^{-(\delta x + \sqrt{\delta x^2 - X^2})\beta/2},$$

where $\delta x = \Delta x_p - \Delta\varepsilon$ and $X = [2\Delta x_p \bar{\Gamma}_0(x_p) \rho(x_p)]^{1/2}$.

3 RESULTS AND DISCUSSION

Figure 1 (middle and bottom panels) shows the results of our calculations of the exciton and plasmon population probability time dynamics as given by the above equations for the first bright exciton in the semiconducting (11,0) carbon nanotube (taken as an example), as the (dimensionless) exciton energy ε is tuned in the vicinity of the nearest (interband) plasmon resonance x_p (E_{11} and P_{11} , respectively, in the top panel of Fig. 1) by means of the QCSE [6]. We used $\Delta\varepsilon = (\hbar/\tau_{ph})(1/2\gamma_0)$

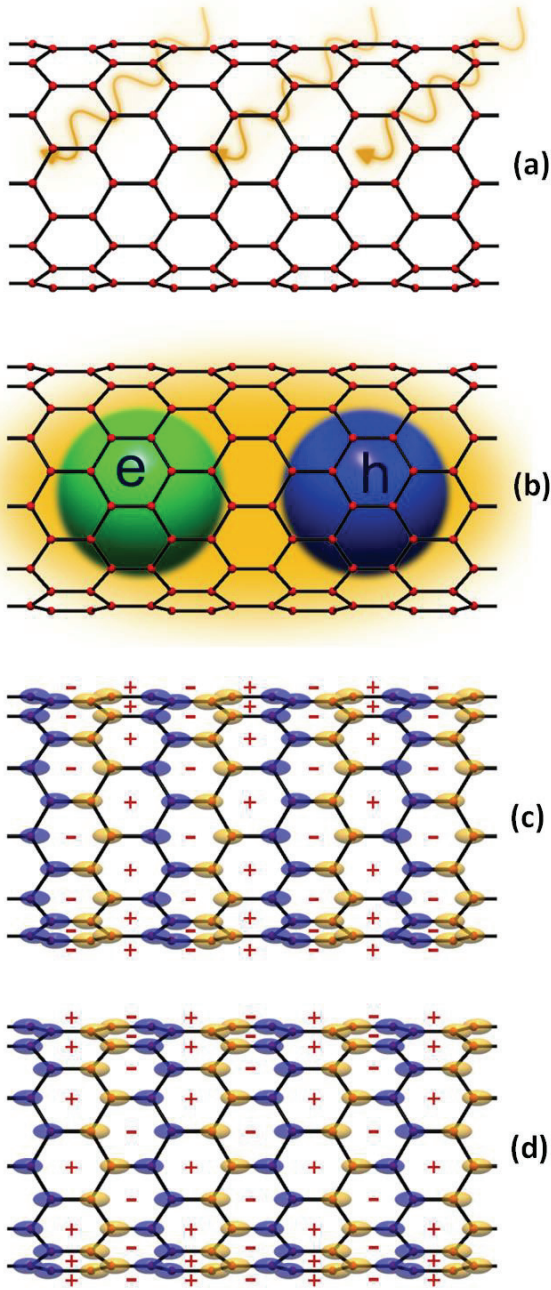


Figure 2: Schematic view of the plasmon generation process by the optically excited exciton. (a),(b) Exciton excitation by the external EM radiation. (c),(d) Plasma oscillations produced by the non-radiative exciton decay can be viewed as standing charge density waves (shown by + and - signs) due to the periodic opposite-phase displacements of the electron shells with respect to the ion cores in the neighboring elementary cells (blue and yellow) on the nanotube surface. Such periodic displacements induce coherent oscillating electric fields of zero mean magnitude, but non-zero mean-square magnitude, concentrated at nanoscale across the nanotube diameter throughout the nanotube length.

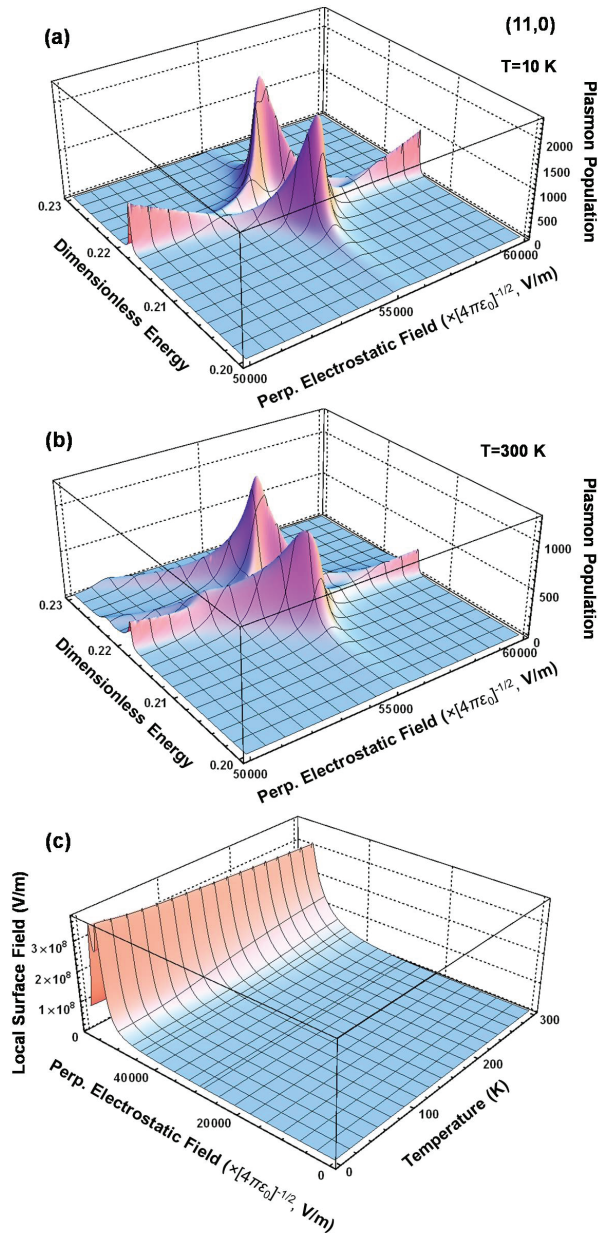


Figure 3: (a),(b) Low- and high-temperature plasmon population (also representing light absorption by excitons) tuned by means of the QCSE using the electrostatic field applied perpendicular to the CN axis. (c) Local surface field amplitude as a function of temperature and perpendicular electrostatic field applied. All calculations are done for the first bright exciton in the (11,0) carbon nanotube.

with the exciton-phonon relaxation time $\tau_{ph} = 30$ fs as reported in Ref. [11]. The plasmon population is seen to increase by at least two orders of magnitude (top line in the bottom panel) under the resonance conditions.

Schematic view of the interband plasmon generation process by the optically excited exciton is shown in Fig. 2. Plasma oscillations produced by the non-radiative exciton decay can be viewed as standing charge density waves due to the periodic opposite-phase displacements of the electron shells with respect to the ion cores in the neighboring elementary cells on the CN surface. Such periodic displacements induce coherent oscillating electric fields of zero mean, but non-zero mean-square magnitude, concentrated at nanoscale across the nanotube diameter throughout the nanotube length.

Figure 3 (a),(b) shows plasmon population numbers averaged over the longitudinal momentum distribution of excitons (also representing light absorption by excitons) calculated at low ($T = 10$ K) and high ($T = 300$ K) temperatures for the first bright exciton in the (11,0) CN exposed to the perpendicular electrostatic field (the QCSE, see Refs. [6],[9] for more details). We see the dramatic increase in the peak intensities, associated with increased optical absorption, when the perpendicular electrostatic field strength exceeds $50000 \times (1/\sqrt{4\pi\epsilon_0})$ V/m, both at low and at high temperatures. Rabi splitting occurs as the field drives the exciton-plasmon system into the strong coupling regime, whereby the effective plasmon generation starts. Temperature generally smoothes the effect due to higher momenta excitons contributing to the process.

Figure 3 (c) demonstrates our result for the calculations of the mean-square surface field associated with plasma oscillations generated by optically excited excitons in the (11,0) CN under the perpendicular electrostatic field applied [9]. Local surface fields $\sim 10^8$ V/m, just a few orders of magnitude less than intra-atomic fields, are created under the resonance conditions. The effect slightly decreases with temperature, but it starts at lower perpendicular electrostatic fields due to higher momenta excitons contributing to the plasmon generation. Strong local surface fields created here are the result of the efficient energy conversion, whereby the external EM radiation energy absorbed to excite excitons transfers into the energy of high-intensity coherent localized optical-frequency fields of charge plasma oscillations on the nanotube surface.

The effect presented here for *individual* single wall carbon nanotubes is analogous to the SPASER effect (Surface Plasmon Amplification by Stimulated Emission of Radiation) reported earlier for *hybrid* metal-semiconductor-dielectric nanostructures [10]. In our case here, surface plasma oscillations and associated coherent local surface fields can be controlled and manipulated by fine tuning the exciton energy in the vicinity of the

plasmon resonance by means of the QCSE. This effect is universal in its physical nature as it originates from the transverse quantization of electronic degrees of freedom in quasi-1D systems. The effect can manifest itself in densely packed aligned nanotube films as well, both through plasmon enhanced inter-tube Casimir interactions, as it is recently demonstrated for double wall CN systems [12], and through the exciton-to-plasmon energy transfer tuned by means of the QCSE. In the latter case, plasmon-induced coherent local surface fields can be used in a variety of new tunable optoelectronic applications both with individual CNs and with nanotube composites, such as enhanced electromagnetic absorption and optical switching, near-field nonlinear-optical probing and sensing, materials nanoscale modification.

4 ACKNOWLEDGMENTS

Supported by NSF (ECCS-1045661 & HRD-0833184), NASA (NNX09AV07A), ARO (W911NF-11-1-0189), and DOE (DE-SC0007117).

REFERENCES

- [1] M.S. Dresselhaus, G. Dresselhaus, R. Saito, and A. Jorio, Annu. Rev. Phys. Chem. 58, 719, 2007.
- [2] I.V. Bondarev, K. Tatur, and L.M. Woods, Optics Communications 282, 661, 2009.
- [3] M. Steiner, et al., Nanoletters 9, 3477, 2010; T. Mueller, et al., Nature Nanotech. 5, 27 2010.
- [4] C.D. Spataru and F. Leonard, Phys. Rev. Lett. 104, 177402, 2010.
- [5] I.V. Bondarev, J. Comp. Theor. Nanosci. 7, 1673, 2010.
- [6] I.V. Bondarev, L.M. Woods, and K. Tatur, Phys. Rev. B 80, 085407, 2009.
- [7] T. Pichler, et al., Phys. Rev. Lett. 80, 4729, 1998; C. Kramberger, et al., Phys. Rev. Lett. 100, 196803, 2008.
- [8] I.V. Bondarev, Phys. Rev. B 83, 153409, 2011; Phys. Status Solidi B 248, 468, 2011; Superlattices and Microstructures 49, 217, 2011.
- [9] I.V. Bondarev, Phys. Rev. B 85, 035448, 2012.
- [10] D.J. Bergman and M.I. Stockman, Phys. Rev. Lett. 90, 027402, 2003.
- [11] V. Perebeinos, J. Tersoff, and Ph. Avouris, Phys. Rev. Lett. 94, 027402, 2005.
- [12] A. Popescu, L.M. Woods, and I.V. Bondarev, Phys. Rev. B 83, 081406(R), 2011.